



HAL
open science

Local light-activation of the Src oncoprotein in an epithelial monolayer promotes collective extrusion

Sarah Moitrier, Nastassia Pricoupenko, Adèle Kerjouan, Christiane I. Oddou, Olivier Destaing, Aude Battistella, Pascal Silberzan, Isabelle Bonnet

► **To cite this version:**

Sarah Moitrier, Nastassia Pricoupenko, Adèle Kerjouan, Christiane I. Oddou, Olivier Destaing, et al.. Local light-activation of the Src oncoprotein in an epithelial monolayer promotes collective extrusion. Communications Physics, 2019, 2 (1), 10.1038/s42005-019-0198-5 . hal-02325048

HAL Id: hal-02325048

<https://hal.science/hal-02325048>

Submitted on 22 Oct 2019

HAL is a multi-disciplinary open access archive for the deposit and dissemination of scientific research documents, whether they are published or not. The documents may come from teaching and research institutions in France or abroad, or from public or private research centers.



L'archive ouverte pluridisciplinaire **HAL**, est destinée au dépôt et à la diffusion de documents scientifiques de niveau recherche, publiés ou non, émanant des établissements d'enseignement et de recherche français ou étrangers, des laboratoires publics ou privés.

ARTICLE

<https://doi.org/10.1038/s42005-019-0198-5>

OPEN

Local light-activation of the Src oncoprotein in an epithelial monolayer promotes collective extrusion

Sarah Moitrier¹, Nastassia Pricoupenko^{1,3}, Adèle Kerjouan^{2,3}, Christiane Oddou^{2,3}, Olivier Destaing^{2,3}, Aude Battistella¹, Pascal Silberzan ¹ & Isabelle Bonnet ¹

Transformed isolated cells are usually extruded from normal epithelia and subsequently eliminated. However, multicellular tumors outcompete healthy cells, highlighting the importance of collective effects. Here, we investigate this situation in vitro by controlling in space and time the activity of the Src oncoprotein within a normal Madin–Darby Canine Kidney (MDCK) epithelial cell monolayer. Using an optogenetics approach with cells expressing a synthetic light-sensitive version of Src (optoSrc), we reversibly trigger the oncogenic activity by exposing monolayers to well-defined light patterns. We show that small populations of activated optoSrc cells embedded in the non-transformed monolayer collectively extrude as a tridimensional aggregate and remain alive, while the surrounding normal cells migrate towards the exposed area. This phenomenon requires an interface between normal and transformed cells and is partially reversible. Traction forces show that Src-activated cells either actively extrude or are pushed out by the surrounding cells in a non-autonomous way.

¹Laboratoire Physico-Chimie Curie, Institut Curie, PSL Research University, Sorbonne Université, CNRS, Equipe labellisée Ligue Contre le Cancer, 75005 Paris, France. ²Institute for Advanced Biosciences, Université Grenoble Alpes, Inserm, CNRS, 38700 La Tronche, France. ³These authors contributed equally: Nastassia Pricoupenko, Adèle Kerjouan, Christiane Oddou, Olivier Destaing. Correspondence and requests for materials should be addressed to I.B. (email: isabelle.bonnet@curie.fr)

During the initial stage of cancer, cell transformation resulting from the activation of oncoproteins and/or inactivation of tumor suppressor proteins, occurs in isolated cells¹. Interactions between transformed cells and their normal neighbors are known to be key regulators not only at the early stage of carcinogenesis, but also later during the tumor progression². Several *in vitro* experiments have looked at the competition between normal and transformed cells by studying sparse transformed cells embedded in a monolayer of normal cells^{3–8}. In these experiments, normal cells are co-cultured with cells expressing cancer-promoting mutations in an inducible manner, such as a temperature shift or an addition of antibiotics. When cells overexpressing an oncogene (H-RasV12³ or v-Src⁴) or the tumor suppressor-knockdown Scribble⁶ are plated with normal Madin-Darby Canine Kidney (MDCK) cells, the isolated transformed cells are either extruded from the monolayer (for Ras or Src cells) or become apoptotic (for Scribble cells). The fate of transformed cells in healthy tissues has been studied *in vivo*, where genetic tools enable the creation of mosaic tissues of transformed cells. In *Drosophila*, Vidal et al. showed that over-activated Src cells were basally extruded and died by apoptosis when they were surrounded by wild-type cells⁹. Similarly, Kajita et al. showed that v-Src expressing cells are apically extruded in zebrafish⁴. Such extrusions are also observed in *Drosophila* and mammals when cells with different growth rates compete¹⁰. In this case, cell fitness drives the elimination of the slower-growing cells. These studies must be put in parallel with others highlighting the suppressive influence of the epithelium on pre-malignant cells to ensure that suboptimal cells do not accumulate during development¹¹.

Despite these advances, the above-mentioned experiments did not control in space or time the transformed population pattern. Powerful optogenetics tools have been used to control gene or protein expression at the single cell level^{12,13} and even at the scale of a group of cells^{14,15}. Here, we take advantage of this strategy to locally tune the oncogenic activation – leading to transformation – in a mammalian cell culture. We focus on Src, which is a membrane-bound tyrosine kinase whose proto-oncogene activity is tightly regulated in normal cells^{16–19}. Src is central in many cellular pathways that are involved in cellular growth, cell–cell and cell–matrix adhesion, motility, and invasion²⁰. Increased levels and activity of Src have been observed in several types of human cancers, and Src has been proposed to induce tumorigenesis through cancer-related pathways^{21–23} by promoting both migration and invasion²⁴. We have chosen to study competition between normal and Src-transformed cells based on (i) Src potential oncogenic activity, (ii) its invasive properties and (iii) its essential role in single cell extrusion⁴.

In the present paper, we question whether collective effects would emerge after a group of contacting cells embedded in a normal monolayer has been transformed. We develop an innovative set-up using optogenetics to control, in time and space, the pattern of oncogenic Src cells, in order to study the competition between a well-defined population of Src cells and their normal neighbors in a monolayer. We show that this local transformation results in the collective extrusion of the group of Src-activated cells from the monolayer. The extruded cells remain alive and appear as a tridimensional aggregate displaying some, but not all, hallmarks of the epithelial-to-mesenchymal transition (EMT). This tissue deformation requires an interface between normal and Src cells and is partially reversible when the light activation is stopped.

Results

The MDCK optoSrc cells. The light-sensitive cryptochrome 2 (CRY2) has been extensively used for optogenetics applications

through blue light-dependent binding to its partner, the truncated cryptochrome-interacting basic-helix-loop-helix (CIBN)^{25,26}. We used a stable MDCK cell line engineered to express a synthetic light-sensitive version of the oncoprotein Src (“optoSrc”) based on the CRY2-CIBN light-gated heterodimerizer system. The optoSrc is a cytosolic potentially active Src mutant that is deprived of membrane anchoring²⁷, this anchoring is required to support the transforming activity of this oncogene. In darkness, the optoSrc is thus inactive in the cytosol. Blue light induces CRY2-CIBN dimerization resulting in the relocalization at the membrane of optoSrc (Fig. 1a, Supplementary Fig. 1)—where it can phosphorylate its physiological substrates and express its oncogenic activity. When blue light is switched off, the CRY2-CIBN dimer splits up: the optoSrc diffuses back to the cytoplasm with a characteristic time of a few minutes^{25,26,28}. To limit the photo-toxicity, MDCK optoSrc cells were exposed to short pulses of blue light which results in efficient activation of the optoSrc. In the following, “blue light” always refers to such pulses of light.

Collective behaviors of activated MDCK optoSrc cells. We first checked that MDCK optoSrc cells, when not exposed to blue light, developed normally into an epithelial monolayer, and had the same phenotype as normal MDCK cells. Blue light did not significantly change the proliferation rate of MDCK optoSrc cells (Supplementary Table 1). This is consistent with the observation that elevated Src is not associated with enhanced proliferation for other cell lines^{29,30}. We also studied the collective migration of MDCK optoSrc cells with a barrier assay (Supplementary Movie 1). In the absence of blue light, these cells migrated collectively as MDCK wild-type with migration fingers preceded by leader cells as previously reported^{31,32}. In contrast, if illuminated with blue light, the MDCK optoSrc monolayer rapidly, within minutes, displayed the characteristics of a migrating monolayer of MDCK cells expressing the activated form of Src³³. The front edge of the monolayer did not display leader cells and migrated 60% faster than a normal MDCK monolayer. Cells at the front edge exhibited membrane ruffles, consistent with the role of Src in adhesion remodeling: Src phosphorylation typically induces actin ruffle formation while disrupting focal adhesions³⁴. We also observed the detachment of individual cells at the front edge of the monolayer. All of these characteristics disappeared when blue-light illumination was stopped.

Effect of blue light on the single-cell extrusion rate. Single-cell extrusion rate in a homogeneous monolayer of identical cells, whether MDCK normal or optoSrc, was not significantly impacted by a global exposition to blue light: the amount of blue light used for photo-activation did not foster single cell extrusions from homogeneous monolayers (Supplementary Fig. 2). In contrast, when we illuminated with blue light a monolayer of normal MDCK cells containing isolated optoSrc cells, the activated optoSrc cells were expelled 15 times more frequently than without illumination (Supplementary Fig. 2). These results are consistent with those previously reported for isolated transformed cells in a normal MDCK monolayer^{3,4}. They also show that single-cell extrusion is caused by the heterogeneity of the cell monolayer.

Local activation of Src results in a collective extrusion. To study the competition between a group of Src cells and their surrounding normal cells, we projected a well-defined pattern of blue light on a homogeneous confluent monolayer of MDCK optoSrc cells (Fig. 1b). We used a Digital Mirror Device (DMD) interfaced with an inverted microscope to project the blue light pattern, which directly defines the cell transformation pattern. Our standard conditions of illumination correspond to a circular pattern

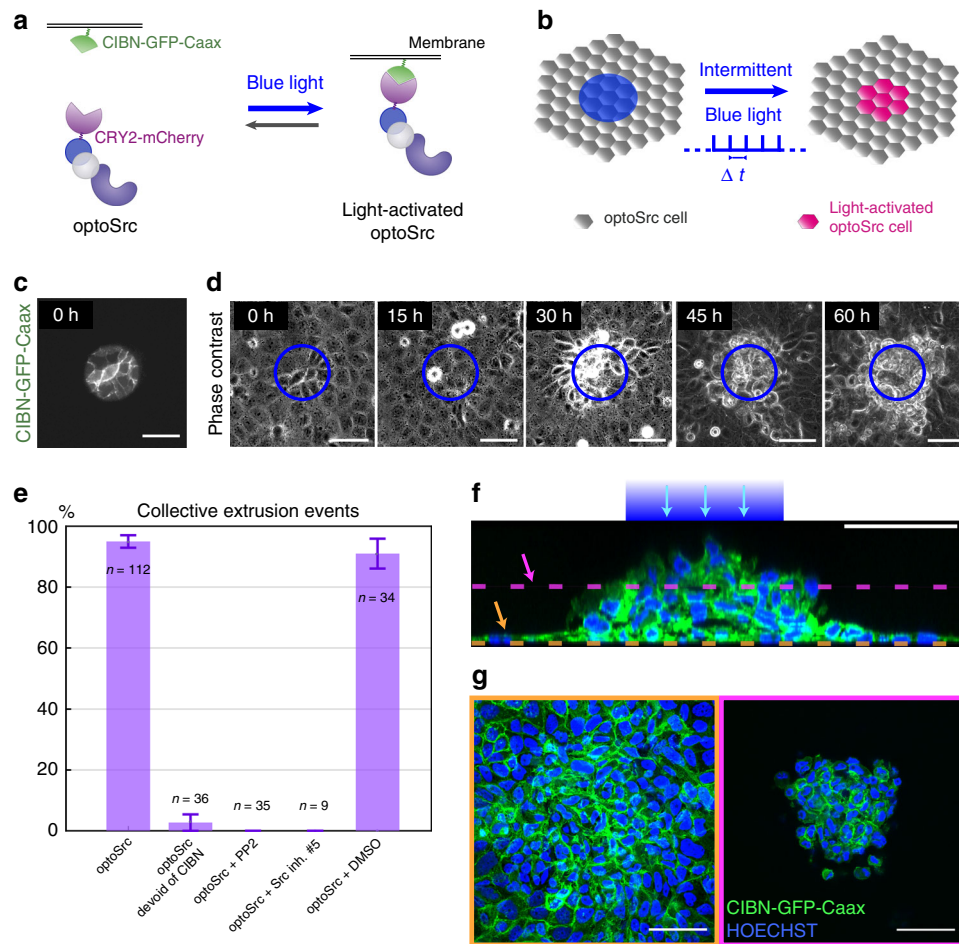


Fig. 1 Collective extrusion triggered by use of light-inducible Src. **a** We use cryptochrome 2 (CRY2) and the truncated cryptochrome-interacting basic-helix-loop-helix (CIBN) light-gated heterodimerizer system to create the optoSrc. In response to blue light, the cytosolic optoSrc relocates to the membrane where it can phosphorylate its substrates. Note that the endogenous Src is present in all the optoSrc cells. **b** By illuminating a monolayer of optoSrc cells with patterned (blue disk) and intermittent (pulses separated by an interval Δt) blue light, we select in time and space the cells to transform. **c, d** A monolayer of Madin-Darby Canine Kidney (MDCK) optoSrc cells is intermittently exposed to blue light (~470 nm pulse of duration 200 ms every $\Delta t = 5$ min) in a circular domain of diameter 70 μm . **c** Only blue-light illuminated cells are displaying CIBN-GFP-Caax. **d** Phase contrast images of the monolayer of MDCK optoSrc cells at different time-points during the blue-light illumination. Time after the start of illumination is indicated in hours and blue circles delineate the region of illumination. At 30 h, the illuminated cells have started to collectively extrude from the monolayer. **e** Number of 3D aggregates formed, in percentage of attempt, depending on the optoSrc construct used, in presence or not of Src inhibitors (PP2 and Src inhibitor #5) for the same conditions of blue-light illumination. The number of attempts n is indicated above each bar, coming from at least 3 different experiments for each condition, except for Src inhibitor #5 (1 experiment). The error bars represent the uncertainty as described in the Methods. **f, g** Confocal images acquired after 60 h of blue-light stimulation. Green: membranes (CIBN-GFP-Caax). Blue: nuclei (Hoechst). **f** Reconstructed side view reveals that extruded cells form a three-dimensional multi-cellular aggregate whose height reached 40 μm . Shaded blue area indicates the original region of illumination. **g** Single confocal slices at the level of the monolayer (left, orange dashed line in **(f)**) and 25 μm above (right, pink dashed line in **(f)**). Scale bars: 50 μm

of diameter 70 μm (Fig. 1c), with a 200-ms pulse of light at 470 nm, every 5 min (Methods). Upon such exposure, cells from the illuminated area extruded simultaneously from the monolayer (Fig. 1d, Supplementary Movie 2). Importantly, these extruded cells remained cohesive and formed an aggregate that grew in size, fed by newly extruded cells as time went on. This phenomenon of “collective extrusion” was observed in 95% of the experiments for which the initial cell density was comprised between 1700 and 3000 cells per mm^2 , and started to occur after 21 ± 10 h (standard deviation (SD), $n = 112$) of illumination in our standard conditions (Fig. 1e).

Contrary to single extruded cells, which readily detach from the monolayer, the 3D cluster made of extruded cells remained well attached to the monolayer, despite the hydrodynamic flows generated by several washing steps. Confocal microscopy confirmed that the extruded aggregate was budding on top of

the monolayer at the location of the blue-light stimulation, or in its close neighborhood (Fig. 1f). Hoechst labeling of the nuclei did not reveal condensed or fragmented chromatin (Fig. 1g), indicating that collectively extruded cells are not apoptotic, contrary to individually extruded cells. The height of the aggregate was $40 \pm 10 \mu\text{m}$ (standard error of the mean (SEM), $n = 12$) after 60 h of blue-light stimulation, corresponding to 210 ± 30 extruded cells (SEM, $n = 6$). Given that there were initially about ten cells in the exposed area, and that the density of non-exposed cells was only multiplied by a factor 3 within the 60 h of the experiment, we conclude that the growth of the aggregate is mostly due to the arrival of new cells and not to proliferation. Tracking of the nuclei during the collective extrusion confirmed that cells extrude simultaneously (Supplementary Movie 3).

Such a collective extrusion was not observed in presence of Src inhibitors (Fig. 1e, Supplementary Fig. 3) or for a homogeneous

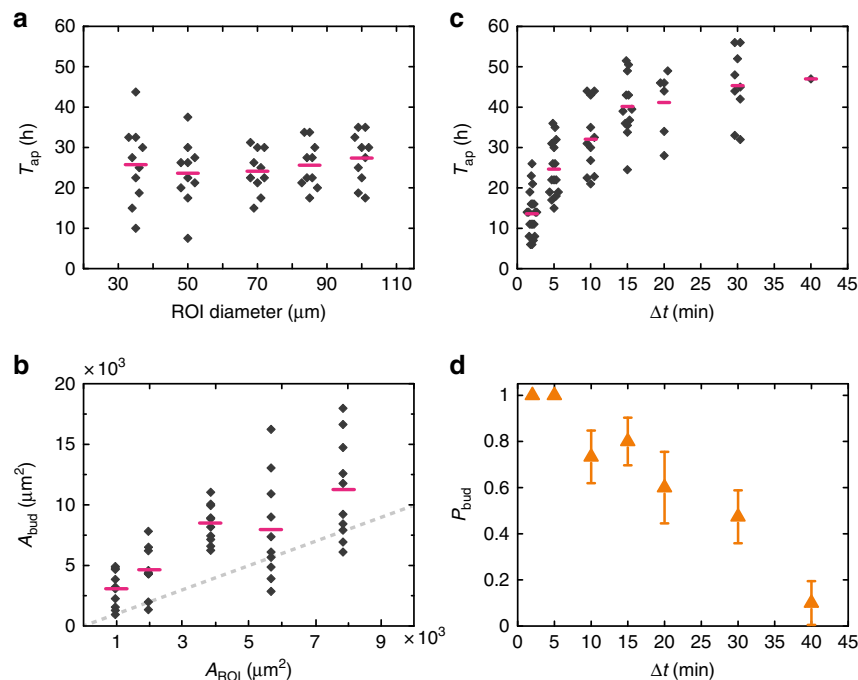


Fig. 2 Control in time and space of the collective extrusion. **a** Appearance time T_{ap} of the collective extrusion as a function of the region of illumination (ROI) diameter when the blue-pulse period Δt is set to 5 min ($n = 10$ samples from 1 experiment for each diameter). **b** Projected area A_{bud} of the aggregate as a function of the area of the ROI A_{ROI} for $\Delta t = 5$ min ($n = 10$ samples from 1 experiment for each diameter). The underlying size of the aggregate is always larger than the ROI. The dashed line indicates $y = x$. **c** Appearance time T_{ap} of the aggregate as a function of Δt for a ROI of diameter $70 \mu\text{m}$. T_{ap} is delayed as the period of blue-light pulses increases, suggesting that varying the amount of optoSrc at the membrane directly impacts the kinetics of the collective extrusion ($n = 20$ for $\Delta t = 2$ min; $n = 15$ for $\Delta t = 5, 10,$ and 15 min; $n = 10$ for $\Delta t = 20$ min; $n = 19$ for $\Delta t = 30$ min and $n = 10$ for $\Delta t = 40$ min, all coming from at least 2 experiments). Horizontal pink lines correspond to mean values in (a–c). **d** Probability of observing a collective extrusion P_{bud} as a function of Δt for a ROI of diameter $70 \mu\text{m}$: the slowed-down kinetics of the collective extrusion when the frequency of blue-light pulses decreases is accompanied with a decrease in collective extrusion events ($n = 20$ for $\Delta t = 2$ min; $n = 15$ for $\Delta t = 5, 10,$ and 15 min; $n = 10$ for $\Delta t = 20$ min; $n = 19$ for $\Delta t = 30$ min and $n = 10$ for $\Delta t = 40$ min, all coming from at least 2 experiments). The error bars represent the uncertainty, as described in the Methods

monolayer of normal MDCK cells illuminated in the same conditions. Moreover, when cell–cell junctions were disrupted with egtazic acid (EGTA), the aggregate could not form. Since the membrane recruitment of Src is essential for its transforming activity³⁵, we also experimented with an optoSrc system deleted of its CIBN component: the recruitment of optoSrc to the membrane was thus not allowed (Supplementary Fig. 1). Upon light-activation, we did not observe collective extrusion for this construct (Fig. 1e), indicating that Src must be over-activated at the membrane to trigger such a collective extrusion. This observation is consistent with the role of Src in the regulation of cell–cell adhesion: in tissue culture, activation of Src is correlated with internalization of cadherin complexes³⁶. In that sense, the collective extrusion could result from a localized decrease of cell–cell adhesions for the group of activated cells embedded in the monolayer.

Control, in time and space, of the collective extrusion. Our set-up allows a good control of the transformed cells in space and time. The DMD allows us to modify the geometry of blue-light pattern projected, while maintaining a constant local light intensity projected on the monolayer. In parallel, we can control the amount of optoSrc at the membrane with the frequency of the blue-light pulses: the less frequent the light pulses, the less time the kinase remains at the membrane and can phosphorylate its substrates^{25,28}.

The area of the blue-light pattern affected the underneath area of the aggregate but not its appearance time (Fig. 2a, b): we find that the underlying area is about 20% larger than the region of

illumination. In contrast, the appearance time T_{ap} of the budding structure, but not its size, was function of the frequency of the pulses: T_{ap} is delayed as Δt increases (Fig. 2c). This reveals that the level of Src at the cells membrane directly affects the kinetics of the collective extrusion: the higher the level of Src activation, the faster the formation of the budding structure. The appearance time as a function of the period Δt of blue light was empirically fitted with a saturation curve $T_{ap} = T_{max} \left(1 - ke^{-\frac{\Delta t}{\tau}} \right)$. We found $T_{max} = 47 \pm 3$ h, $k = 0.9 \pm 0.1$, and $\tau = 9 \pm 3$ min. This characteristic time τ is larger than the previously reported CIBN/CRY2 dissociation time of ~ 3 min^{25,28}. We conclude that τ is a time constant of the integrated behavior of the cells, a cumulative effect in time of the over-activation of Src, and possibly, its downstream effectors. The plateau of $T_{ap}(\Delta t)$ at long times logically coincides with a decrease of the probability to observe collective extrusion events (Fig. 2d). The value of T_{max} around 50 h suggests that if collective extrusion has not occurred during the first 50 h of blue-light stimulation, it is unlikely to happen at all. Hence, the frequency of the blue light is a key parameter controlling the kinetics of the appearance of the aggregate.

Since we control in time and space the collective extrusion process by tuning the area of illumination and the frequency of stimulation, our optogenetics-based system is thus a powerful in vitro tool to trigger, on-demand, the formation of a 3D aggregate of transformed cells in a normal epithelial monolayer.

Molecular markers of the collective extrusion. Tissue crowding has been shown to favor cell delamination in epithelial tissues^{37–40}.

To investigate the role of crowding in the collective extrusion phenomenon, we measured the probability P_{bud} of observing the formation of a 3D aggregate during the first 60 h of stimulation, as a function of the initial cell density (Supplementary Fig. 4). For initial densities d_i corresponding to confluent MDCK optoSrc cells monolayer ($1700 \text{ cells per mm}^2 \leq d_i \leq 3000 \text{ cells per mm}^2$), P_{bud} was high (95%, $n = 112$). If the monolayer of MDCK optoSrc cells was initially below confluence ($700 \text{ cells per mm}^2 \leq d_i \leq 1700 \text{ cells per mm}^2$), P_{bud} was reduced by half, suggesting that a minimal amount of surrounding cells is needed. Surprisingly, when density was too high at the beginning of blue-light stimulation ($d_i \geq 3000 \text{ cells per mm}^2$), the probability of budding was also reduced ($P_{\text{bud}} \sim 0.7$).

Since P_{bud} does not correlate directly with cell density, we looked for molecular changes between MDCK optoSrc cells that were stimulated or not. F-actin strongly accumulates in exposed cells, as revealed by live-imaging of SiR-actin during collective extrusion (Fig. 3a, b and Supplementary Fig. 5). This actin recruitment suggests that a contractile mechanism is at play in the collective extrusion process. However, the distribution of myosin was diffuse in the budding structure (Supplementary Fig. 5), ruling out the presence of a supracellular actomyosin cable that would drive the extrusion. Logically, treatment with calyculin A (resp. Y-27632) which increases (resp. decreases) cell contractility accelerated (resp. delayed) the average appearance time (Fig. 3c). In parallel, we performed immunostaining of monolayers of MDCK optoSrc cells either fully exposed or not exposed. Upon blue-light illumination, E-cadherin loses its localization at the membrane and accumulates in the cytoplasm, in agreement with previous observations showing that elevated expression of active Src disrupts E-cadherin localization⁴¹. Besides, vimentin was enriched in the stimulated cells (Supplementary Fig. 6). Similar trends were observed in collectively extruded aggregates (Fig. 3d, e). Down-regulation of E-cadherin and expression of vimentin have already been observed in other cell lines for which c-Src is elevated⁴². Furthermore, during single Src-transformed cell extrusion, vimentin has been shown to accumulate at the interface between normal and transformed cells⁴. A relocalization of E-cadherin from the plasma membrane to the cytoplasm and an increase of vimentin expression are both hallmarks of the EMT. However, this transition from an epithelial phenotype to a mesenchymal phenotype appears to be only partial, not least because the level of E-cadherin at junctions remains high enough to ensure a good adhesion between extruded cells.

Role of the surrounding non-activated cells. While cells in the exposed pattern collectively extruded, the surrounding cells converged towards the region of stimulation (Fig. 4a, Supplementary Movie 4). We measured that a $70 \mu\text{m}$ -diameter region of illumination induced a convergent flow of non-exposed cells in a $150 \mu\text{m}$ -wide disk around the collective extrusion (Fig. 4b, c). The presence of this convergent cell flow during illumination suggests that the local activation triggers a long-range response mediated by cell–cell interactions and these migrating cells feed the extruded cluster. Turning off the illumination once the 3D structure was formed reversed the flow of cells (from the extrusion site outwards) and the cells of the extruded cluster reintegrated the monolayer (Fig. 4a, Supplementary Movie 4). This observation not only demonstrated that the process of collective extrusion was partially reversible, but also confirmed that extruded cells were still alive.

To test if collective extrusion results from interaction between the two cell types, we shed blue light on optoSrc cells confined on a circular adhesive pattern^{43,44} that matched the area of light stimulation. When the whole confined MDCK optoSrc

monolayer was fully illuminated with blue light, collective extrusion events were observed in only 10% of the cases (Fig. 4d, $n = 10$ samples from 2 different experiments) instead of 95% for non-confined monolayers, for an initial cell density comprised between 1700 and 3000 cells per mm^2 in both cases. This confirms our hypothesis that collective extrusion requires the presence of wild-type cells surrounding the populations of Src cells.

Traction forces point away from the activated Src cluster.

Regarding the mechanical contribution involved in collective extrusion, we consider three possible scenarios compatible with the observed convergent cell flow (Fig. 5a–c). In the first scenario, the activated optoSrc cells collectively contract and “pull” the surrounding monolayer inwards (Fig. 5a). The second scenario is the opposite situation where the surrounding normal cells actively “push” on the group of activated optoSrc cells (Fig. 5b). In the last scenario, the group of activated optoSrc cells is actively escaping from the monolayer (Fig. 5c), which prompts the surrounding monolayer to migrate inwards to cover the surface released by this process⁴⁵. Some of these scenarios can be distinguished by measuring the traction forces exerted by the cells on their substrate during the collective extrusion⁴⁶. These forces were measured by Traction Force Microscopy (TFM)^{47,48}. For these experiments, the MDCK optoSrc monolayer was grown on a fibronectin-coated polyacrylamide gel of Young modulus $\sim 10 \text{ kPa}$ loaded with fluorescent beads. Note that the TFM technique requires a soft substrate, while we generally carried out experiments on glass. Although collective extrusion is slowed down on a fibronectin-coated polyacrylamide gel of $\sim 10 \text{ kPa}$, the final outcome is globally unchanged. From the analysis of the beads’ displacements, we concluded that the traction forces were highest at the interface between the two populations, and directed outwards (Fig. 5d–f). Two hypotheses are compatible with such a force map. In the first one, the collective extrusion would be a non-autonomous process in which the surrounding cells actively migrate towards the exposed area and effectively push the Src cells out of the monolayer (Fig. 5b). The second scenario would correspond to an active extrusion of the Src cells that would release new area for the surrounding normal cells to migrate on (Fig. 5c). We note that the flow and traction force patterns measured during collective extrusion are similar to those measured during single cell extrusion⁴⁹, but at a supra-cellular scale.

Discussion

Optogenetics enabled us to activate the oncoprotein Src in mammalian tissue culture with a good control in space and time. We created mosaic tissues by over-activating Src in well-defined subpopulations in an epithelial monolayer, giving rise to two interacting cell populations. We find that groups of activated optoSrc cells collectively extrude from the monolayer giving rise to 3D aggregates. These spheroid-like structures remained strongly attached to the monolayer (resisting hydrodynamic flows) and were not observed in presence of EGTA, which disrupts cell–cell junctions. Altogether, these observations point to a new phenomenon of “collective extrusion”. Collective extrusion requires a surrounding monolayer and the recruitment of Src at the membrane.

We note that the cells in the aggregate differ in the number of pulses they received. The cells that have been more exposed to blue light are more likely to be the first to extrude. They are located at the top of the aggregate and exhibit a high expression of vimentin. The cells that entered last into the region of illumination do not immediately extrude, and they still have sufficient

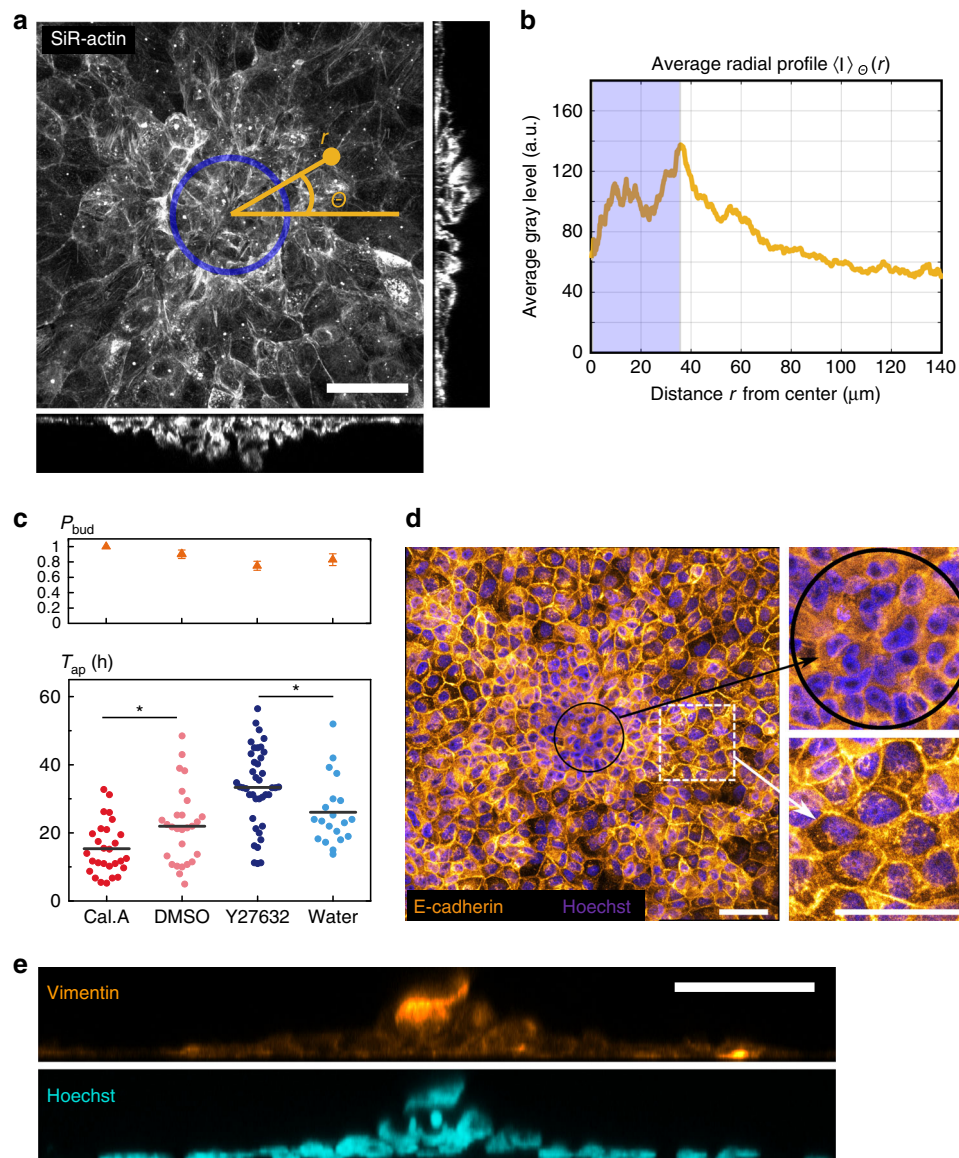


Fig. 3 Molecular changes associated with the collective extrusion. **a** Confocal image of F-actin after 60 h of blue-light illumination. Maximum intensity projection of a Z-stack of 32 slices with 1 μm slice interval with orthogonal views from the confocal stack. The blue circle delineates the region of blue-light illumination. (r, θ) are the polar coordinates used for averaging in **(b)**. **b** Average radial profile of the gray value of the image depicted in **(a)**. The blue shaded area indicates the region of stimulation. **c** Effect of drugs modifying contractility on the probability of budding P_{bud} and the appearance time T_{ap} . Calyculin A (1 nM) decreases T_{ap} ($p = 0.021$, Wilcoxon rank sum test) and increases P_{bud} , while Y27632 (10 μM) increases T_{ap} ($p = 0.013$, Wilcoxon rank sum test) and decreases P_{bud} . Horizontal black lines correspond to the mean values. The error bar of P_{bud} is the uncertainty as described in the Methods ($n_{\text{Cal}} = 28$, $n_{\text{DMSO}} = 30$, $n_{\text{Y27632}} = 55$ and $n_{\text{water}} = 24$, all coming from at least 3 different experiments). **d**, **e** A monolayer of Madin-Darby Canine Kidney (MDCK) optoSrc cells was subjected to the standard conditions of illumination for 60 h and fixed with paraformaldehyde. **d** Immunostaining for E-cadherin (orange) in a monolayer displaying a budding aggregate reveals that E-cadherin is depleted from the membrane for Src-activated cells (black circle) compared to non-illuminated cells (dashed white square). Cell nuclei were stained with Hoechst (purple). **e** Reconstructed side view of a confocal acquisition after an immunostaining for vimentin (orange) in a monolayer of MDCK optoSrc cells displaying a budding aggregate. Vimentin is strongly expressed in the cells at the top of the budding structure, compared to cells in the monolayer. Cell nuclei were stained with Hoechst (cyan). Scale bars: 50 μm

level of E-cadherin at the membrane to ensure strong attachment of the aggregate to the monolayer.

Previous work has evidenced the extrusion of individual Src-expressing cells dispersed in a normal monolayer⁴: these single-cell extrusions share common features with the collective extrusion we report here. First, in both single and collective extrusion, cells are extruded apically (towards the lumen). Second, it occurs in an apoptosis-independent manner. Third, it happens only when transformed cells are surrounded by

normal cells. However, there are two major differences between collective and single extrusion processes. First, the collective extrusion is reversible. Second, contrary to single-cell extrusion, where cells are weakly attached to the monolayer (and often dissociate from it), the collectively extruded cells remain alive and form a cohesive spheroid strongly attached to the underlying substrate. We hypothesize that the collective extrusion protects the extruded cells as a group and prevents cell death.

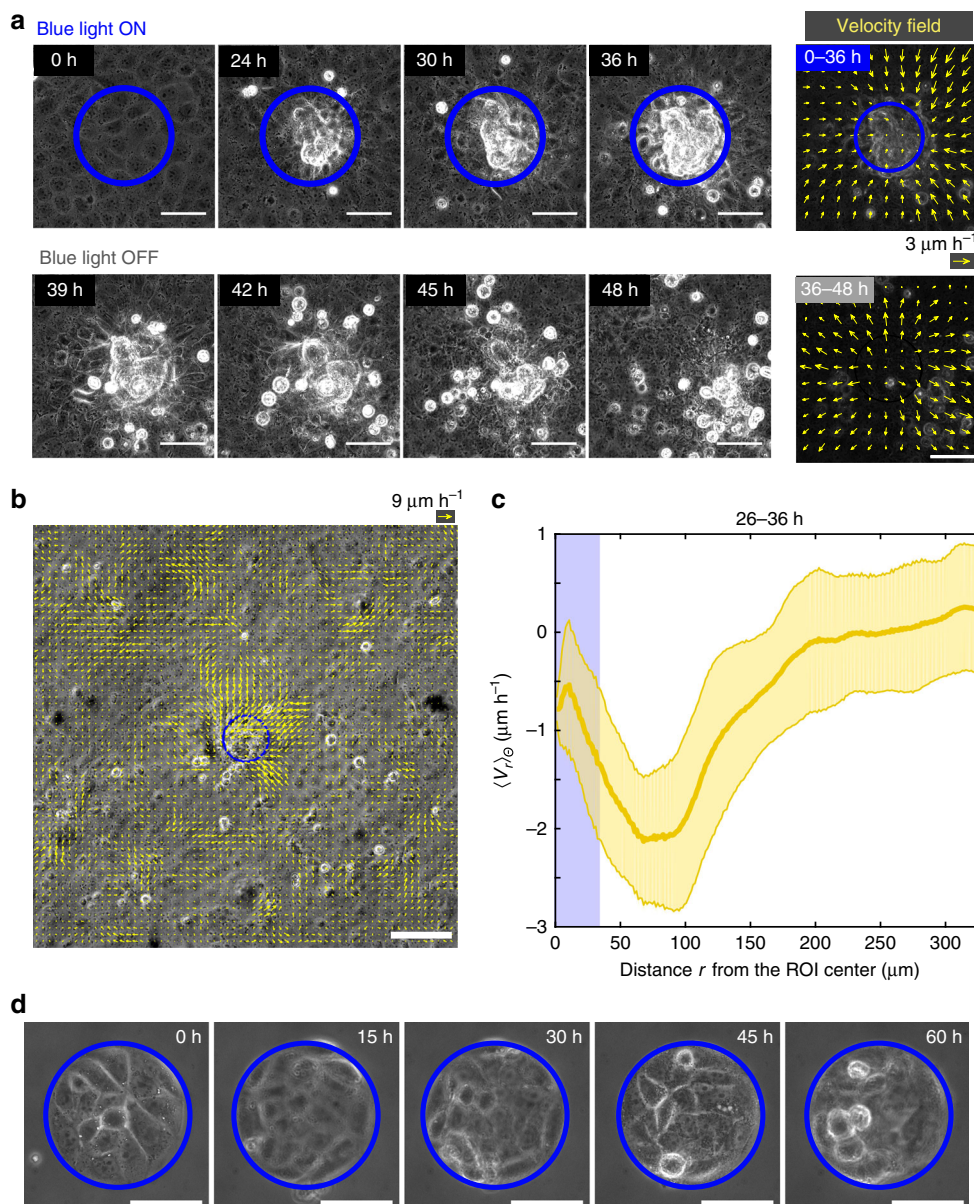


Fig. 4 Cell flow during the collective extrusion. **a** ON/OFF blue-light illumination of a monolayer of Madin-Darby Canine Kidney (MDCK) optoSrc cells in a circular domain. Blue light is switched ON for 36 h inside the blue circle, then switched OFF from 36 h until 48 h. Phase contrast images at different time-points and time-averaged velocity field (yellow arrows). When the blue light is ON, the collective extrusion occurs within 24 h and the corresponding velocity field obtained by particle image velocimetry (PIV) analysis shows the convergent flow of cells during this period. From $t = 36$ h, the blue light is turned OFF, and most of the cells forming the bud reintegrated the monolayer, showing that collective extrusion is partially reversible. The corresponding velocity field is reversed. Scale bars: 50 μm . **b** Velocity field (yellow arrows) averaged between 26 h and 36 h (when the velocities in the monolayer are the highest) after the start of illumination for a collective extrusion observed at low-magnification. For this experiment, the appearance time is $T_{\text{ap}} = 28 \pm 2$ h. The blue circle delineates the region of illumination (circle of diameter 70 μm). Scale bar: 100 μm . **c** Angular average of the radial component of the velocity field displayed in **(b)**. The convergent flow extends about 150 μm away from the center of the region of illumination, indicated by the blue area. The error bars indicate the standard deviation. **d** Phase contrast images of a monolayer of MDCK optoSrc cells confined in a circular domain that corresponds to the region of illumination (blue circle) at different time-points after the start of illumination, time is indicated in hours. Scale bars: 50 μm .

Cell density has been identified as the main parameter controlling single cell extrusion in various studies in epithelia^{39,49,50}. In our case, at high cell density, we measured a decrease of P_{bud} in parallel with the apparition of clusters of optoSrc-CRY2 in the cytoplasm (Supplementary Fig. 4). To account for this surprising result, we propose that cell crowding favors the homodimerization of CRY2 to the detriment of the CRY2/CIBN dimerization⁵¹. This would limit the recruitment and over-

activation of optoSrc at the membrane. At very low density, blue light stimulation of optoSrc cells did not result in extrusion but in a completely different outcome: an islet of a few optoSrc cells exposed to blue light quickly (within a couple of hours) spreads out and breaks apart like mesenchymal cells (Supplementary Fig. 7), which is consistent with the fact that over-activation of Src induces an EMT^{23,52}. In the 3D-aggregate of extruded cells, the relocalization of E-cadherin and up-regulation of vimentin

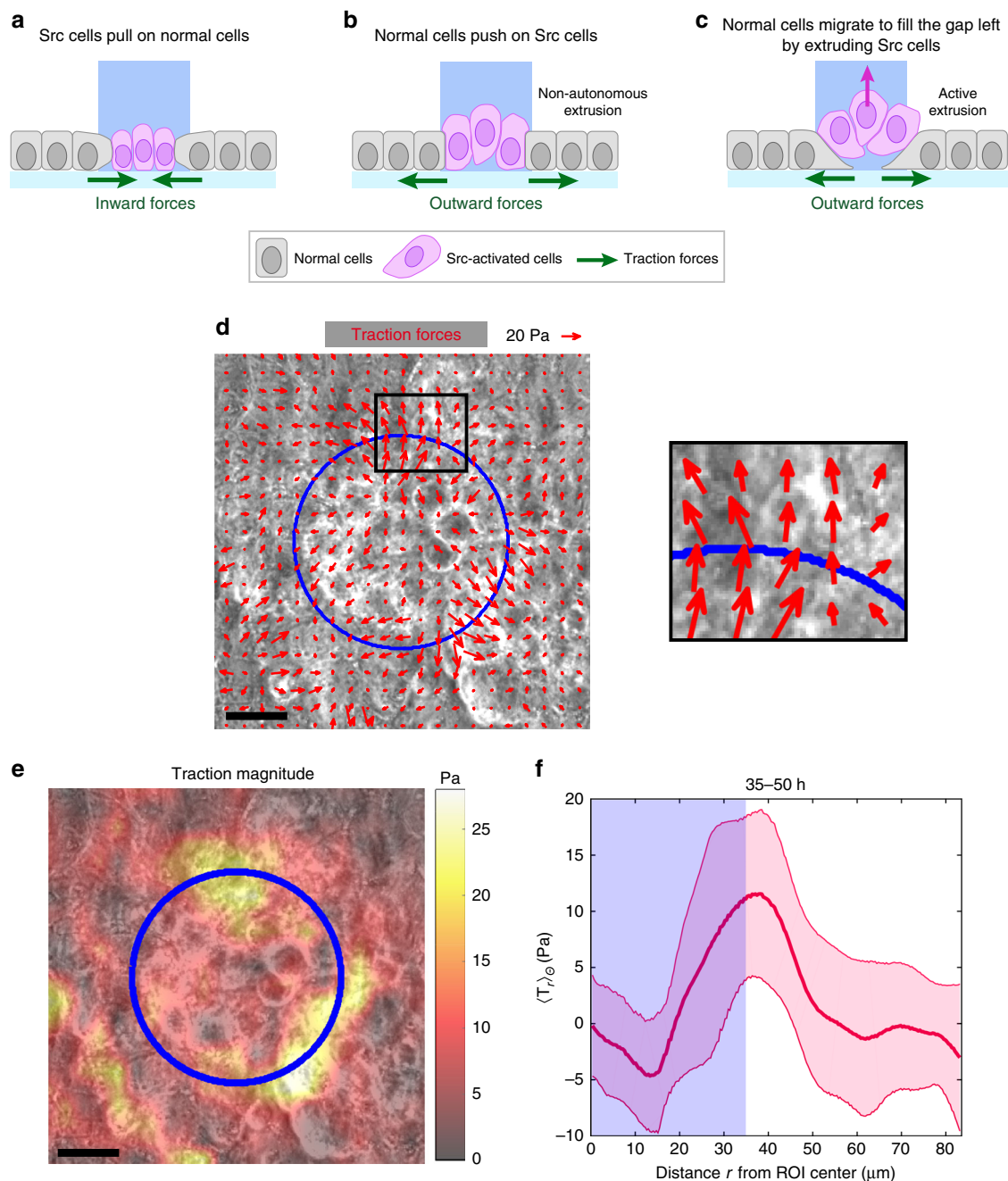


Fig. 5 Traction forces during the collective extrusion. **a–c** Three scenarios for the mechanical contribution involved in collective extrusion. **a** The illuminated optoSrc cells contract and pull the surrounding monolayer inwards. The resulting forces on the substrate would be directed inwards. **b** The non-exposed monolayer is actively pushing on the group of activated optoSrc cells. In such non-autonomous extrusion, we expect the forces generated on the substrate to be directed outwards. **c** The group of optoSrc cells is actively escaping the monolayer, which closes the resulting gap by migrating inwards. The forces generated are also expected to be directed outwards. **d–f** Traction force microscopy experiment during the collective extrusion. **d** Traction forces (red arrows) averaged between 35 h and 50 h after the start of illumination and overlaid with phase image. The region delineated with the black rectangle is blown up on the right. Note the direction of the forces away from the region of stimulation (indicated by the blue circle). **e** Magnitude of the traction force field displayed in **(d)**, color-coded (Pa) and overlaid on the phase image. **f** Angular average of the radial component, of the traction force field displayed in **(d)**. The blue area indicates the region of stimulation (diameter 70 μm). The error bars indicate the standard deviation. Scale bars: 50 μm

supports the idea that the extruded cells are likely undergoing an EMT-like process, albeit maintaining a cohesive structure. In this context, it would be of particular interest to confirm this analysis by studying other EMT markers, such as snail or beta-catenin to get a complete characterization of the Src-activated cells.

Collective extrusion requires a frontier between two populations which have different Src levels at the membrane. The tissue deformation therefore results from the interactions between these

two populations. Recent studies have demonstrated the importance of mechanical forces in the competition that takes place between normal and transformed epithelial cells^{37,53,54}. We showed that the traction forces are pointing outwards at the interface between the two cell populations, while the surrounding normal cells converge towards the aggregate and eventually get incorporated in it. A non-autonomous extrusion process for which surrounding normal cells actively push the Src cells is

compatible with such a force map. It is interesting to note that pathological cyst formation in *Drosophila* imaginal discs has also been proposed to be a non-autonomous process⁵⁵. However, in that case, the tissue deformation is triggered by the interface contractility between two distinct cell populations.

Very recently, Messal et al. analyzed how clusters of Kras-transformed cells trigger morphological changes in tissue architecture of pancreatic ducts⁵⁶. Our results are consistent with their observation of endophytic lesions made of transformed cells growing inwards for ducts of large diameter. Although tumor formation is a complex multifactorial process, we show here that a group of contacting Src-activated cells is enough to create a tumor-like aggregate. Since Src is known to be involved in tumor cell dissemination⁵⁷, the ability to create clusters of Src-activated cells on demand using an epithelial cell line is a valuable tool to investigate the role of Src activity in tumor dissemination.

More generally, our results show how tridimensional cellular aggregates can develop by collective extrusion from an epithelial monolayer, based on the simultaneous transformation of a group of neighboring cells, which are extruded but thrive as a collective. Such photo-inducible models may also allow for the study of biological processes that involve partial and reversible EMT, as it has been observed in circulating tumor cell clusters (micro metastases)—in which partial EMT of cancer cells has been associated with increased metastatic properties^{58,59}.

Methods

Cell culture. The optoSrc construct refers to the OptoSrc + CIBN-GFP-Caax described in another of our publication²⁷. Madin-Darby Canine Kidney (MDCK) and MDCK optoSrc cells were both cultured in Dulbecco's Modified Eagle's Medium (DMEM) supplemented with 1% Penicillin-Streptomycin and 10% (vol/vol) fetal bovine serum (all from Gibco) at 37 °C, 5% vol CO₂ and 95% relative humidity. Cells were seeded in 6-well glass bottom plates (IBL, Austria) at roughly 0.5 million cells per well, and left to incubate overnight. For time-lapse acquisition, DMEM was replaced with FluoroBrite DMEM (Gibco) - to reduce medium autofluorescence - similarly supplemented with Penicillin-Streptomycin and fetal bovine serum, but not with GlutaMAX.

Population doubling time and single-cell extrusion rate. Cells were either not exposed or exposed to blue light using our standard conditions of illumination in complete DMEM. For the population doubling time T , cells were manually counted at six different time-points between $t = 0$ (seeding time) and $t = 60$ h over 5 fields of view for each conditions (1 movie). T was estimated by fitting the number of cells as a function of time t with the equation $n_0 2^{t/T}$ where n_0 was the initial number of cells (Supplementary Table 1). For homogeneous monolayers (made of one cell type), extrusions were counted in a $150 \times 150 \mu\text{m}^2$ region for six samples (2 movies) over 40 ± 3 h after the confluence. For mixed monolayers, extrusion rate was defined as the proportion of isolated cells that have been extruded in the span of 60 h (Supplementary Fig. 2).

Microscopy. Time-lapse acquisitions were performed on an inverted microscope (Zeiss Axiovert 200 M) equipped with a temperature, CO₂ and humidity regulation (Life Imaging Services, Switzerland), a motorized stage for multipositioning (Marzhauser, Germany) and a CCD camera (CoolSnap HQ2 from Photometrics, USA or Retiga R6 from QImaging, Canada). A $40\times/0.75\text{NA}/\text{Ph}2$ objective (Olympus, Japan) was used, and images were taken every 15 min for 60 h. Phase and fluorescence light sources were, respectively, a pE-100 and a pE-300-white (CoolLed, UK). Image acquisition was computer controlled with Metamorph (Molecular Devices, USA). For confocal observation, the monolayers were observed with a LSM880 NLO with a $40\times/1.3 \text{ OIL}/\text{DIC II PL APO VIS-IR}$ or a $63\times/1.4 \text{ OIL}/\text{DIC II PL APO}$ objectives (Zeiss, Germany). For live imaging of F-actin, we used SiR-Actin (Spirochrome) at 100 nM supplemented with verapamil (10 μM). For live imaging of nuclei, we used SiR-DNA (Spirochrome) at 2 μM .

Blue-light activation. Blue-light patterned illumination was made using a Mosaic2 (Andor, UK) coupled to a X-Cite XLED (Lumen Dynamics, BDX LED module 450-495 nm) using the GFP filters (excitation filter BP 450-490 nm and dichroic mirror FT 510) and controlled with the "Mosaic Targeted Illumination" Metamorph plugin. Unless otherwise mentioned, the illuminated region was a disk of diameter 70 μm and the intermittent illumination consisted of a 200-ms pulse of blue light every $\Delta t = 5$ min. For these standard conditions of illumination, the light power was measured to be 20 μW after the objective, with a PM30 optical powermeter (Thorlabs, US). Given that the characteristic dissociation time of the

complex CRY2/CIBN is ~ 3 min^{25,28}, setting $\Delta t = 5$ min ensures a moderate level of CRY2 at the membrane. The photo-activation parameters (region size, frequency and pulse duration) were controlled using custom Metamorph journals. Three pulse durations were tested (50, 200 and 400 ms): since the duration of the pulse did not obviously change the apparition time of the collective extrusion (Supplementary Fig. 8), we choose to set it to 200 ms, the lowest value that enables a correct GFP imaging.

Drugs. PP2 (Sigma), Src inhibitor #5 (Biaffin GmbH) and calyculin A (Life technologies) were dissolved in dimethyl sulfoxide (DMSO) and added to the medium to reach a final concentration of 10 μM , 10 nM, and 1 nM, respectively. The control wells were supplemented with equivalent volumes of DMSO. Y-27632 (Sigma) and egtazic acid (EGTA, Euromedex) were diluted in distilled water and used at a final concentration of 10 μM and 2 mM, respectively. The drugs were added when medium was changed, between 1 and 4 h preceding the beginning of the photoactivation, and left for the duration of the experiment.

Preparation of the adhesive patterns. The detailed protocol for adhesive patterns can be found in others of our publications^{43,44}. Briefly, plasma-cleaned glass slides were first PEGylated with a robust surface treatment. Domains were defined by photolithography directly on the cell-repellent coating in such a way that it remained protected by the photoresist everywhere except at the desired location of the adhesive domains. Using the photoresist as a mask, the polyethylene glycol (PEG) coating was etched on the photoresist-free areas with a plasma cleaner, revealing the underlying glass. The resist was then dissolved away leading to clean glass domains surrounded by PEG-coated glass.

Image analysis. The appearance time T_{ap} of the bud was evaluated by eye on the phase contrast images, with an uncertainty of ± 2 h, as the moment in which the first budding cell starts to emerge from the monolayer, in conjunction with an apparent convergence of the monolayer towards the activated region. Single extruded cells that did not subsequently belong to the 3D structure were not considered. The initial density was determined by manually counting the number of cells in the field of view for the first frame of the acquisition. Image processing was performed with custom ImageJ macros⁶⁰ and Matlab (MathWorks, US) scripts. The number of cells in the bud were counted on 3D confocal images, by automatic segmentation of cell nuclei using the surface tool in Imaris (Bitplane, UK). Tracking of nuclei labelled with SiR-DNA was done manually with the cell counter Image J plugin.

Immunostaining. Cells were fixed for 10 min in 4% paraformaldehyde (Euro-medex) and permeabilized for 4 min using 0.1% Triton X-100 in phosphate-buffered saline (PBS) with 0.1% bovine serum albumin (BSA, all reactants from Sigma). The cells were then blocked in a solution of 2.5% normal goat serum (NGS, Santa Cruz) in PBS-BSA for 1 h, incubated with the selected primary antibody (references below) for 1 h and washed with PBS. They were then incubated with the secondary antibody (references below) for 30 min at room temperature, washed with PBS, Hoechst-labeled (NucBlue Live ready Probes, ThermoFisher) and mounted on glass slides using ProLong Gold (Life technologies). Primary antibodies: E-cadherin (BD Biosciences, 610181, mouse at a concentration of 1:100); vimentin (Dako M0725 clone V9, mouse at a concentration of 1:300); p-MLC (Cell signaling 3674, rabbit at a concentration of 1:100). Secondary antibodies: goat anti-mouse A633 (Molecular Probes); goat anti-rabbit (Sigma, SAB4600141) both at a concentration of 1:1000.

Particle image velocimetry (PIV). PIV was used to analyze the velocity fields in the cell monolayers^{61,62} using the MatPIV toolbox for Matlab (Mathworks, US). The window size was set to 64 pixels ($\sim 23 \mu\text{m}$), with an overlap of 0.25. Sliding average over 10 h was performed.

Traction force microscopy (TFM). The protocol for TFM was adapted from Tse et al.⁶³. Briefly, coverslips were plasma-cleaned for 10 min, treated with 3-aminopropyltrimethoxysilane (2% vol/vol in isopropanol, Sigma) and glutaraldehyde (0.5% vol/vol in ddH₂O, Sigma), then dried with compressed air. These coverslips are referred to as "activated". In parallel, microscope glass slides were incubated with fibronectin bovine protein (Gibco) in phosphate-buffered saline (PBS) at 25 μg per mL for 30 min at room temperature, then rinsed with PBS and left to air dry. We then made a gel of Young's modulus 10 kPa by mixing 40% acrylamide solution, 2% bis-acrylamide solution (Bio-Rad) and 1% (vol/vol) of fluorescent beads (FluoSpheres 0.2 μm dark red fluorescent (660/680), Life technologies). Ammonium persulfate (1% vol/vol, Bio-Rad) and TEMED (1% vol/vol, Bio-Rad) were added to this mix to start the polymerization of the acrylamide gel. Then 30 μL of the solution was applied on the fibronectin-coated glass slide immediately after drying, and an "activated" coverslip was placed on top. During the polymerization, the gel attaches covalently to the activated surface on one side, and attaches to the fibronectin proteins on the other side. This step, inspired by the deep-UV patterning technique⁶⁴, allows to coat the surface of the gel with fibronectin. When the polymerization was complete, the sandwiched gel was immersed

in PBS, and the fibronectin-coated glass slide was carefully detached from the gel. The gel was then thoroughly rinsed with PBS and incubated in culture medium for 45 min at 37 °C, before the cells were seeded on it, and left to adhere overnight. The coverslip bearing the gel was then placed under the microscope in a POCmini-2 cell cultivation system (Pecon GmbH). At the end of the experiment, the cells were carefully detached from the gel using trypsin (TrypLE, Gibco), to take the reference image of the beads at rest. To compute the traction forces, we used the TFM Fiji plugin available online⁶⁵.

Probability of observing a collective extrusion. The probability of observing a collective extrusion was defined as $P_{\text{bud}} = \frac{k}{n}$, where k is the number of occurrences of the collective extrusion observed over n experiments. We consider the binomial distribution with parameters n and $p = \frac{P_{\text{bud}}}{100}$. The confidence interval for p was estimated using $\sqrt{\frac{p(1-p)}{n}}$.

Reporting Summary. Further information on research design is available in the Nature Research Reporting Summary linked to this article.

Data availability

The data that support the findings of this study are available from the corresponding author upon reasonable request.

Received: 12 February 2019 Accepted: 31 July 2019

Published online: 26 August 2019

References

- Hanahan, D. & Weinberg, R. A. Hallmarks of cancer: the next generation. *Cell* **144**, 646–674 (2011).
- Hogan, C. Impact of interactions between normal and transformed epithelial cells and the relevance to cancer. *Cell. Mol. Life Sci.* **69**, 203–213 (2012).
- Hogan, C. et al. Characterization of the interface between normal and transformed epithelial cells. *Nat. Cell Biol.* **11**, 460–467 (2009).
- Kajita, M. et al. Interaction with surrounding normal epithelial cells influences signalling pathways and behaviour of Src-transformed cells. *J. Cell Sci.* **123**, 171–180 (2010).
- Kon, S. et al. Cell competition with normal epithelial cells promotes apical extrusion of transformed cells through metabolic changes. *Nat. Cell Biol.* **19**, 530–541 (2017).
- Norman, M. et al. Loss of Scribble causes cell competition in mammalian cells. *J. Cell Sci.* **125**, 59–66 (2012).
- Kajita, M. & Fujita, Y. EDAC: Epithelial defence against cancer–cell competition between normal and transformed epithelial cells in mammals. *J. Biochem.* **158**, 15–23 (2015).
- Wu, S. K. et al. Cortical F-actin stabilization generates apical–lateral patterns of junctional contractility that integrate cells into epithelia. *Nat. Cell Biol.* **16**, 167–178 (2014).
- Vidal, M., Larson, D. E. & Cagan, R. L. Csk-deficient boundary cells are eliminated from normal *Drosophila* epithelia by exclusion, migration, and apoptosis. *Dev. Cell* **10**, 33–44 (2006).
- Levayer, R. & Moreno, E. Mechanisms of cell competition: themes and variations. *J. Cell Biol.* **200**, 689–698 (2013).
- Leung, C. T. & Brugge, J. S. Outgrowth of single oncogene-expressing cells from suppressive epithelial environments. *Nature* **482**, 410–413 (2012).
- Tischer, D. & Weiner, O. D. Illuminating cell signalling with optogenetic tools. *Nat. Rev. Mol. Cell Biol.* **15**, 551–558 (2014).
- Zhang, K. & Cui, B. Optogenetic control of intracellular signaling pathways. *Trends Biotechnol.* **33**, 92–100 (2015).
- Valon, L., Marin-Llaurado, A., Wyatt, T., Charras, G. & Trepat, X. Optogenetic control of cellular forces and mechanotransduction. *Nat. Commun.* **9**, 14396 (2017).
- Izquierdo, E., Quinkler, T. & De Renzis, S. Guided morphogenesis through optogenetic activation of Rho signalling during early *Drosophila* embryogenesis. *Nat. Commun.* **9**, 2366 (2018).
- Rous, P. A sarcoma of the fowl transmissible by an agent separable from the tumor cells. *J. Exp. Med.* **13**, 397–411 (1911).
- Stehelin, D., Varmus, H. E., Bishop, J. M. & Vogt, P. K. DNA related to the transforming gene(s) of avian sarcoma viruses is present in normal avian DNA. *Nature* **260**, 170–173 (1976).
- Hunter, T. & Sefton, B. M. Transforming gene product of Rous sarcoma virus phosphorylates tyrosine. *Proc. Natl Acad. Sci. USA* **77**, 1311–1315 (1980).
- Collett, M. S. & Erikson, R. L. Protein kinase activity associated with the avian sarcoma virus src gene product. *Proc. Natl Acad. Sci. USA* **75**, 2021–2024 (1978).
- Brown, M. T. & Cooper, J. A. Regulation, substrates and functions of src. *Biochim. Biophys. Acta* **1287**, 121–149 (1996).
- Biscardi, J. S., Tice, D. A. & Parsons, S. J. c-Src, receptor tyrosine kinases, and human cancer. *Adv. Cancer Res.* **76**, 61–119 (1999).
- Summy, J. M. & Gallick, G. E. Src family kinases in tumor progression and metastasis. *Cancer Metastas. Rev.* **22**, 337–358 (2003).
- Boyer, B., Bourgeois, Y. & Poupon, M.-F. Src kinase contributes to the metastatic spread of carcinoma cells. *Oncogene* **21**, 2347–2356 (2002).
- Parsons, S. J. & Parsons, J. T. Src family kinases, key regulators of signal transduction. *Oncogene* **23**, 7906–7909 (2004).
- Kennedy, M. J. et al. Rapid blue-light-mediated induction of protein interactions in living cells. *Nat. Methods* **7**, 973–975 (2010).
- Idevall-Hagren, O., Dickson, E. J., Hille, B., Toomre, D. K. & De Camilli, P. Optogenetic control of phosphoinositide metabolism. *Proc. Natl Acad. Sci. USA* **109**, E2316–E2323 (2012).
- Kerjouan, A. et al. Molecular flux control encodes distinct cytoskeletal responses by specifying SRC signaling pathway usage. *bioRxiv* 648030 (2019). <https://doi.org/10.1101/648030>.
- Valon, L. et al. Predictive spatiotemporal manipulation of signaling perturbations using optogenetics. *Biophys. J.* **109**, 1785–1797 (2015).
- Jones, R. J. et al. Elevated c-Src is linked to altered cell–matrix adhesion rather than proliferation in KM12C human colorectal cancer cells. *Br. J. Cancer* **87**, 1128–1135 (2002).
- Welman, A. et al. Increases in c-Src expression level and activity do not promote the growth of human colorectal carcinoma cells in vitro and in vivo. *Neoplasia* **8**, 905–916 (2006).
- Poujade, M. et al. Collective migration of an epithelial monolayer in response to a model wound. *Proc. Natl Acad. Sci. USA* **104**, 15988–15993 (2007).
- Reffay, M. et al. Orientation and polarity in collectively migrating cell structures: statics and dynamics. *Biophys. J.* **100**, 2566–2575 (2011).
- Platek, A. et al. v-Src accelerates spontaneous motility via phosphoinositide 3-kinase, phospholipase C and phospholipase D, but abrogates chemotaxis in Rat-1 and MDCK cells. *J. Cell Sci.* **117**, 4849–4861 (2004).
- Hamadi, A., Deramaut, T. B., Takeda, K. & Rondé, P. Src activation and translocation from focal adhesions to membrane ruffles contribute to formation of new adhesion sites. *Cell. Mol. Life Sci.* **66**, 324–338 (2009).
- Cross, F. R., Garber, Ea, Pellman, D. & Hanafusa, H. A short sequence in the p60src N terminus is required for p60src myristylation and membrane association and for cell transformation. *Mol. Cell Biol.* **4**, 1834–1842 (1984).
- Gavard, J. & Gutkind, J. S. VEGF controls endothelial-cell permeability by promoting the β -arrestin-dependent endocytosis of VE-cadherin. *Nat. Cell Biol.* **8**, (2006).
- Wagstaff, L. et al. Mechanical cell competition kills cells via induction of lethal p53 levels. *Nat. Commun.* **7**, 11373 (2016).
- Marinari, E. et al. Live-cell delamination counterbalances epithelial growth to limit tissue overcrowding. *Nature* **484**, 542–545 (2012).
- Eisenhoffer, G. T. et al. Crowding induces live cell extrusion to maintain homeostatic cell numbers in epithelia. *Nature* **484**, 546–549 (2013).
- Levayer, R., Dupont, C. & Moreno, E. Tissue crowding induces caspase-dependent competition for space. *Curr. Biol.* **26**, 670–677 (2016).
- Avizienyte, E. et al. Src-induced de-regulation of E-cadherin in colon cancer cells requires integrin signalling. *Nat. Cell Biol.* **4**, 632–638 (2002).
- Mandal, M. et al. Epithelial to mesenchymal transition in head and neck squamous carcinoma. *Cancer* **112**, 2088–2100 (2008).
- Deforet, M., Hakim, V., Yevick, H. G., Duclos, G. & Silberzan, P. Emergence of collective modes and tri-dimensional structures from epithelial confinement. *Nat. Commun.* **5**, 3747 (2014).
- Duclos, G. et al. in *Methods in Molecular Biology* (ed. Gautreau, A.) **1749**, 387–399 (Springer, New York, 2018).
- Cochet-Escartin, O., Ranft, J., Silberzan, P. & Marcq, P. Border forces and friction control epithelial closure dynamics. *Biophys. J.* **106**, 65–73 (2014).
- Brugués, A. et al. Forces driving epithelial wound healing. *Nat. Phys.* **10**, 683–690 (2014).
- Style, R. W. et al. Traction force microscopy in physics and biology. *Soft Matter* **10**, 4047 (2014).
- Tseng, Q. et al. Spatial organization of the extracellular matrix regulates cell–cell junction positioning. *Proc. Natl Acad. Sci. USA* **109**, 1506–1511 (2012).
- Kocgozlu, L. et al. Epithelial cell packing induces distinct modes of cell extrusions. *Curr. Biol.* **26**, 2942–2950 (2016).
- Saw, T. B. et al. Topological defects in epithelia govern cell death and extrusion. *Nature* **544**, 212–216 (2017).
- Duan, L. et al. Understanding CRY2 interactions for optical control of intracellular signaling. *Nat. Commun.* **8**, 547 (2017).
- Behrens, J. et al. Loss of epithelial differentiation and gain of invasiveness correlates with tyrosine phosphorylation of the E-cadherin/beta-catenin complex in cells transformed with a temperature-sensitive v-SRC gene. *J. Cell Biol.* **120**, 757–766 (1993).

53. Rodríguez-Franco, P. et al. Long-lived force patterns and deformation waves at repulsive epithelial boundaries. *Nat. Mater.* **16**, 1029–1037 (2017).
54. Moitrier, S. et al. Collective stresses drive competition between monolayers of normal and Ras-transformed cells. *Soft Matter* **15**, 537–545 (2019).
55. Bielmeyer, C. et al. Interface contractility between differently fated cells drives cell elimination and cyst formation. *Curr. Biol.* **26**, 563–574 (2016).
56. Messal, H. A. et al. Tissue curvature and apicobasal mechanical tension imbalance instruct cancer morphogenesis. *Nature* **566**, 126–130 (2019).
57. Leroy, C. et al. Quantitative phosphoproteomics reveals a cluster of tyrosine kinases that mediates Src invasive activity in advanced Colon Carcinoma. *Cells* <https://doi.org/10.1158/0008-5472.CAN-08-2354> (2009).
58. Jolly, M. K. et al. Implications of the hybrid epithelial/mesenchymal phenotype in metastasis. *Front. Oncol.* **5**, 155 (2015).
59. Aiello, N. M. et al. EMT subtype influences epithelial plasticity and mode of cell migration. *Dev. Cell* **45**, 681–695.e4 (2018).
60. Rasband, W. S. ImageJ, U. S. National Institutes of Health.
61. Petitjean, L. et al. Velocity fields in a collectively migrating epithelium. *Biophys. J.* **98**, 1790–1800 (2010).
62. Deforet, M. et al. Automated velocity mapping of migrating cell populations (AVeMap). *Nat. Methods.* **9**, 1081–1083 (2012).
63. Tse, J. R. & Engler, A. J. Preparation of hydrogel substrates with tunable mechanical properties. *Curr. Protoc. cell Biol.* **10**, Unit 10.16 (2010).
64. Azioune, A., Carpi, N., Tseng, Q., Théry, M. & Piel, M. Protein micropatterns: A direct printing protocol using deep UVs. *Methods Cell Biol.* **97**, 133–146 (2010).
65. TFM plugins. Available at: <https://sites.google.com/site/qingzongtseng/tfm>.

Acknowledgements

We thank A. Buguin and the members of the Biology-inspired Physics at MesoScales group for fruitful discussions. We acknowledge F. Cayrac (cell sorting), S. DeBeco (reagents), F. Saiag (electronics) and R. Fert and E. Nicolau (mechanics). We thank PICT-IBiSA (member of France-Bioimaging, ANR-10-INBS-04) of the UMR3215 as well as the flow cytometry core facility of Institut Curie. This work was funded by the GEFLUC Ile de France, the C’Nano Ile de France, and the Labex CelTisPhyBio, La Ligue

and an ANR-JCJC « invadocontrol ». S.M. was funded by an IPGG PhD grant and A.K. was supported by doctoral fellowships from La Ligue and FRM.

Author contributions

I.B. designed research; S.M, N.P. and A.B. performed the experiments; A.K., C.O. and O.D. constructed the optoSrc cell lines; S.M., P.S., and I.B. analyzed data; S.M, P.S. and I.B. wrote the paper and all the authors contributed to discussion.

Additional information

Supplementary information accompanies this paper at <https://doi.org/10.1038/s42005-019-0198-5>.

Competing interests: The authors declare no competing interests.

Reprints and permission information is available online at <http://npg.nature.com/reprintsandpermissions/>

Publisher’s note: Springer Nature remains neutral with regard to jurisdictional claims in published maps and institutional affiliations.



Open Access This article is licensed under a Creative Commons Attribution 4.0 International License, which permits use, sharing, adaptation, distribution and reproduction in any medium or format, as long as you give appropriate credit to the original author(s) and the source, provide a link to the Creative Commons license, and indicate if changes were made. The images or other third party material in this article are included in the article’s Creative Commons license, unless indicated otherwise in a credit line to the material. If material is not included in the article’s Creative Commons license and your intended use is not permitted by statutory regulation or exceeds the permitted use, you will need to obtain permission directly from the copyright holder. To view a copy of this license, visit <http://creativecommons.org/licenses/by/4.0/>.

© The Author(s) 2019